ORIGINAL ARTICLE

Plant, Cell & Environment   PCE   WILEY

Leaves as bottlenecks: The contribution of tree leaves to hydraulic resistance within the soil−plant−atmosphere continuum

Brett T. Wolfe[1,2] | Matteo Detto[2,3] | Yong-Jiang Zhang[4] |
Kristina J. Anderson-Teixeira[2,5] | Tim Brodribb[6] | Adam D. Collins[7] |
Chloe Crawford[1] | L. Turin Dickman[7] | Kim S. Ely[8] | Jessica Francisco[1] |
Preston D. Gurry[1] | Haigan Hancock[1] | Christopher T. King[1] |
Adelodun R. Majekobaje[1] | Christian J. Mallett[1] | Nate G. McDowell[9,10] |
Zachary Mendheim[1] | Sean T. Michaletz[11] | Daniel B. Myers[1] | Ty J. Price[1] |
Alistair Rogers[8] | Lawren Sack[12] | Shawn P. Serbin[8] | Zafar Siddiq[13] |
David Willis[1] | Jin Wu[14,15] | Joseph Zailaa[5,12,16] | S. Joseph Wright[2]

[1]School of Renewable Natural Resources, Louisiana State University Agricultural Center, Baton Rouge, Louisiana, USA

[2]Smithsonian Tropical Research Institute, Balboa, Republic of Panama

[3]Department of Ecology and Evolutionary Biology, Princeton University, Princeton, New Jersey, USA

[4]School of Biology and Ecology, University of Maine, Orono, Maine, USA

[5]Conservation Ecology Center, Smithsonian's National Zoo & Conservation Biology Institute, Front Royal, Virginia, USA

[6]School of Natural Sciences, University of Tasmania, Hobart, Australia

[7]Los Alamos National Laboratory, Earth and Environmental Sciences Division, Los Alamos, New Mexico, USA

[8]Brookhaven National Laboratory, Environmental and Climate Science Department, Upton, New York, USA

[9]Pacific Northwest National Lab, Atmospheric Sciences and Global Change Division, Richland, Washington, USA

[10]School of Biological Sciences, Washington State University, Pullman, Washington, USA

[11]Department of Botany and Biodiversity Research Centre, University of British Columbia, Vancouver, British Columbia, Canada

[12]Department of Ecology and Evolutionary Biology, University of California, Los Angeles, California, USA

[13]Department of Botany, Government College University, Lahore, Pakistan

[14]School of Biological Sciences, Research Area of Ecology and Biodiversity, The University of Hong Kong, Hong Kong, China

[15]State Key Laboratory of Agrobiotechnology, The Chinese University of Hong Kong, Hong Kong, China

[16]School of the Environment, Yale University, New Haven, Connecticut, USA

Correspondence
Brett T. Wolfe, School of Renewable Natural Resources, Louisiana State University Agricultural Center, Baton Rouge, Louisiana 70803, USA.
Email: bwolfe@agcenter.lsu.edu

Abstract

Within vascular plants, the partitioning of hydraulic resistance along the soil-to-leaf continuum affects transpiration and its response to environmental conditions. In trees, the fractional contribution of leaf hydraulic resistance (R_{leaf}) to total soil-to-leaf hydraulic resistance (R_{total}), or fR_{leaf} (=R_{leaf}/R_{total}), is thought to be large, but this has not been tested comprehensively. We compiled a multibiome data set of fR_{leaf} using new and previously published measurements of pressure differences within trees in situ. Across 80 samples, fR_{leaf} averaged 0.51 (95% confidence interval

[CI] = 0.46−0.57) and it declined with tree height. We also used the allometric relationship between field-based measurements of soil-to-leaf hydraulic conductance and laboratory-based measurements of leaf hydraulic conductance to compute the average fR_{leaf} for 19 tree samples, which was 0.40 (95% CI = 0.29−0.56). The in situ technique produces a more accurate descriptor of fR_{leaf} because it accounts for dynamic leaf hydraulic conductance. Both approaches demonstrate the outsized role of leaves in controlling tree hydrodynamics. A larger fR_{leaf} may help stems from loss of hydraulic conductance. Thus, the decline in fR_{leaf} with tree height would contribute to greater drought vulnerability in taller trees and potentially to their observed disproportionate drought mortality.

1 | INTRODUCTION

Transpiration from terrestrial plants is a fundamental component of Earth's water cycle. Transpired water flows under tension through a hydraulic continuum that extends from soil to leaves within the soil–plant–atmosphere continuum (SPAC) (Sperry et al., 2002; Venturas et al., 2017). When water flow through the SPAC is impeded, such as during droughts, stomata close, slowing transpiration, carbon dioxide uptake and plant growth (Anderegg et al., 2020; Schwalm et al., 2017). Plants invest in roots, stems, and leaves presumably to maximize fitness, including growth, but multiple tradeoffs limit the capacity for water uptake and transport. For example, mechanical strength and water storage tradeoff with hydraulic transport capacity within woody tissues (Pratt et al., 2021; Scholz et al., 2011). Likewise, within whole plants, variation in branching architecture has opposing effects on light interception and SPAC hydraulic efficiency (Smith et al., 2014) and allocation to leaves increases both productivity and susceptibility to hydraulic failure during droughts (Trugman et al., 2019).

Several models predict how plant traits and environmental conditions influence SPAC fluxes including transpiration (e.g., Christoffersen et al., 2016; Sperry et al., 2002). These SPAC models are becoming integral components of Earth system models that predict feedbacks between ecosystems and the atmosphere (Fisher et al., 2018). Central to SPAC modelling is how hydraulic resistance (i.e., the pressure difference per water flux) is partitioned among components along the hydraulic continuum, that is, rhizosphere, roots, stems, and leaves (Sperry et al., 1998). In trees, most of the SPAC pathlength is in roots and stems, whereas leaves have a relatively short pathlength. Yet, leaf hydraulic resistance (R_{leaf}) can be relatively high, as water passes through small xylem conduits and living cells. Consequently, the fraction of total SPAC hydraulic resistance (R_{total}) within leaves, or fR_{leaf} ($=R_{leaf}/R_{total}$), may be outsized.

To date, the most comprehensive analysis of fR_{leaf} among plant species is that of Sack et al. (2003). They combined data from several studies, including herbs, woody seedlings and saplings, and mature trees and shrubs. A standardized major axis (SMA) fit through the log-transformed values of leaf hydraulic conductance (K_{leaf}) as a function of total-SPAC hydraulic conductance (K_{total}) had a slope of 1.21 (95% confidence interval [CI] = 0.99−1.43), an intercept of log(4.2), and $r = 0.91$ (Sack et al., 2003). Since resistance is the inverse of conductance, this result suggests that leaves consistently contribute about 25% (i.e., 1/4.2) of the total SPAC hydraulic resistance (i.e., fR_{leaf} = ca. 0.25). This scaling relationship suggests a general convergence among plants in hydraulic architecture and function: leaves contribute a disproportionately high amount of hydraulic resistance for their relatively short pathlength in the SPAC, acting as hydraulic bottlenecks.

However, among the plants analysed by Sack et al. (2003), the mature trees and shrubs do not fit the overall SMA as well as the herbs, seedlings, and saplings. Indeed, we fit an SMA through the 11 samples of mature trees and shrubs within the data set of Sack et al. (2003) and found a slope of 1.01 (95% CI = 0.51−1.99), intercept of log(2.22), and $r = 0.25$. This analysis suggests that fR_{leaf} is generally higher (i.e., ca. 0.45) and more variable (i.e., lower r) in mature trees and shrubs than in herbs, seedlings, and saplings. Similarly, studies that have inferred fR_{leaf} in situ from pressure differences between soil, stems, and leaves on apricot trees, orange trees, loblolly pine trees, and seasonally dry tropical forest trees have found fR_{leaf} of 0.3−0.8 (Alarcón et al., 2003; Brodribb et al., 2002; Domec et al., 2009; Moreshet et al., 1990). fR_{leaf} may also decline with tree size. For example, von Allman et al. (2015) predicted that fR_{leaf}

decreased from ca. 0.40 to 0.18 among maple and oak trees with trunk diameters 5–30 cm.

Variation in fR$_{leaf}$ is expected to affect plant performance. As soil and air dry, reduced plant water potential (Ψ) is associated with loss of hydraulic conductance (K) in roots, stems, and leaves, which can be described with Ψ$_{50}$, that is, the Ψ at which an organ loses 50% of K (Venturas et al., 2017). In trees, the loss of stem K (K$_{stem}$) beyond critical thresholds is associated with drought mortality (Adams et al., 2017). The 'hydraulic segmentation' hypothesis of Zimmerman (1983) predicts that higher fR$_{leaf}$ buffers stem Ψ (Ψ$_{stem}$) during droughts, protecting trees from K$_{stem}$ loss. Similarly, the 'vulnerability segmentation' hypothesis of Tyree et al. (1991) predicts that when leaf Ψ$_{50}$ is high relative to stem Ψ$_{50}$, K$_{leaf}$ loss slows transpiration and buffers Ψ$_{stem}$, protecting trees from K$_{stem}$ loss. Here, we illustrate these hypotheses using a simple model of water transport that assumes plants regulate transpiration to avoid SPAC hydraulic failure (Sperry et al., 2016). We ran several simulations of a soil dry down while varying hydraulic segmentation (i.e., fR$_{leaf}$) and vulnerability segmentation (i.e., relative values of leaf vs. stem Ψ$_{50}$) (Figure 1). During the dry down, Ψ$_{stem}$ increased with fR$_{leaf}$ (i.e., the slope in Figure 1e), illustrating the hydraulic segmentation hypothesis. Likewise, for any given fR$_{leaf}$, trees with vulnerability segmentation (leaf Ψ$_{50}$ > stem Ψ$_{50}$) maintained higher Ψ$_{stem}$ (i.e., the difference in elevation between curves in Figure 1e). In nature, both mechanisms are likely to occur to varying degrees among tree species. Both mechanisms cause reduced K$_{total}$ and transpiration during water deficit (Figure 1a,c,g,h), which represents a tradeoff between hydraulic safety and productivity. However, when leaves and stems are equally vulnerable (leaf Ψ$_{50}$ = stem Ψ$_{50}$), modelled K$_{total}$ and transpiration were insensitive to fR$_{leaf}$ (open symbols in Figure 1g,h). In this case, a tradeoff for high fR$_{leaf}$ is unapparent.
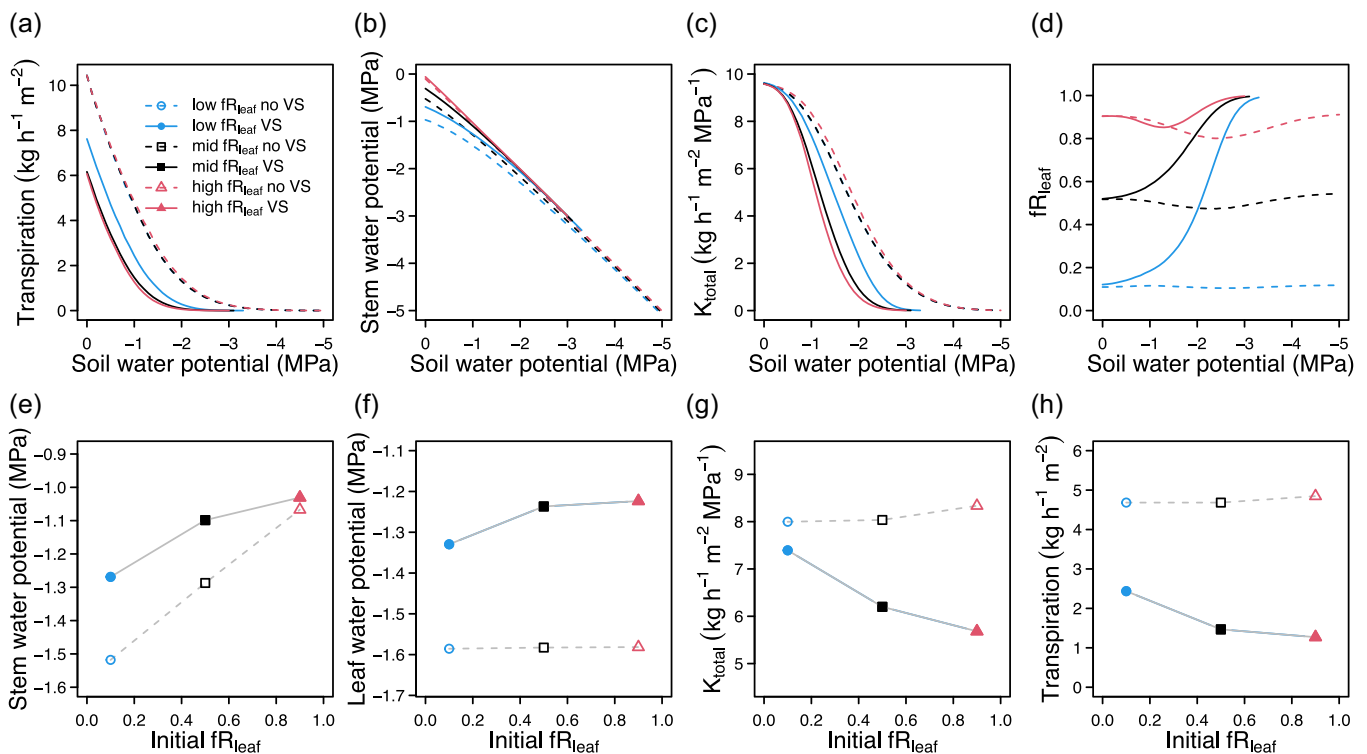
FIGURE 1 Effects of varying fR$_{leaf}$ within the hydraulic transport model of Sperry et al. (2016). The model was parameterised with a single soil layer that dried from 0 to −5 MPa while vapour pressure deficit was 1 kPa. Root and stem Ψ$_{50}$ were set to −2 MPa. Leaf Ψ$_{50}$ was set to −2.0 (i.e., no vulnerability segmentation (no VS)) and −1.0 MPa (i.e., VS). fR$_{leaf}$ was set to 0.1, 0.5, and 0.9 (i.e., low, mid, and high fR$_{leaf}$). The legend in panel (a) is a key to the six combinations of fR$_{leaf}$ and VS for all panels. Everything else was held constant, particularly the initial K$_{total}$, which here represents the total investment in the plant hydraulic system. Thus, higher fR$_{leaf}$ represents a relative increase in allocation to hydraulic conductance in roots and stems and a relative decrease in allocation to hydraulic conductance in leaves. As soil water potential declined, transpiration (a), stem water potential (b), and K$_{total}$ (c) declined at rates that varied with initial fR$_{leaf}$ and VS. Within plants, fR$_{leaf}$ changed during the dry down as leaves, stems and roots lost hydraulic conductance at varying rates (d). Panels (e-h) show a single point during the dry down, when soil water potential was −1 MPa. Trees with VS maintained higher stem water potential than trees without VS and, with or without VS, stem water potential increased with fR$_{leaf}$ (e). Similarly, trees with VS maintained higher leaf water potential than trees without VS, whereas effect of varying fR$_{leaf}$ on leaf water potential small (f). With VS, K$_{total}$ (g) and transpiration (h) declined with higher fR$_{leaf}$.

Given that fR_{leaf} likely affects tree performance and that its variation among trees is not well understood, we assessed fR_{leaf} in trees from various biomes and habitats. We estimated fR_{leaf} from previously reported and new measurements of pressure differences in situ within tropical and temperate trees. We also followed Sack et al. (2003) in exploring the K_{total}–K_{leaf} allometry with an expanded data set of trees. We compared methods for estimating fR_{leaf} in trees and tested whether fR_{leaf} varies among biomes, clades (conifers vs. angiosperms), tree sizes, and with soil moisture. We also addressed the hydraulic segmentation hypothesis by testing whether trees with higher fR_{leaf} maintained higher Ψ_{stem}.

2 | MATERIALS AND METHODS

2.1 | Estimating fR_{leaf} from pressure differences

According to Darcy's Law, the water flux (F) through a system is equal to the pressure difference between endpoints divided by its hydraulic resistance. In transpiring trees, around midday, the hydraulic resistance between soil and leaf (R_{total}) is:

$$R_{total} = (\Psi_{soil} - \Psi_{leaf\_md} - h\rho_w g)/F \qquad (1)$$

where Ψ_{soil} and Ψ_{leaf_md} are soil and midday leaf water potential, respectively, and $h\rho_w g$ is the hydrostatic gravitational pressure, where h is tree height, ρ_w is the density of water and g is gravitational acceleration (Domec et al., 2009; Whitehead, 1998).

The F term in Equation 1 can be measured with several techniques. Transpiration from individual leaves can be measured with a porometer or portable leaf gas-exchange system to estimate leaf-area-specific R_{total} (MPa mmol^{-1} m^2 s). However, estimating F with leaf-level measurements is generally problematic because of the difficulty in matching boundary layer conditions between measurement chambers and ambient conditions, where they are highly variable temporally within and among tree canopies (Pearcy et al., 1989). F can also be measured within roots, trunks, and branches with sap flow probes (e.g., Granier, 1985). These measurements are generally scaled by cross-sectional area of the measured organ or by the whole tree. They can be converted to give leaf-area-specific R_{total} through allometric relationships or by directly measuring whole-tree leaf area.

One assumption in Equation 1 is that midday F is in a steady state (i.e., F is at equilibrium within the SPAC). This assumption does not hold when water stored within the plant is in flux. However, the contribution of stored water to F is generally negligible around midday as water stored within plant tissues enters the transpiration stream in the morning and is recharged with soil water in the afternoon and night (Goldstein et al., 1998; Loustau et al., 1998; Maherali & DeLucia, 2001).

Ψ_{soil} in the rooting zone is often estimated with predawn leaf water potential (Ψ_{leaf_pd}) as:

$$\Psi_{soil} = \Psi_{leaf\_pd} + h\rho_w g \qquad (2)$$

Equation 2 relies on the assumption that, except for the hydrostatic gravitational pressure difference, Ψ_{leaf_pd} is in equilibrium with Ψ_{soil}. This assumption has theoretical support if low nighttime vapour pressure deficit (VPD) and closed stomata combine to drive F to zero. However, when R_{total} is very high, nighttime VPD is high, or nighttime stomatal conductance is high, then Ψ_{leaf_pd} and Ψ_{soil} do not equilibrate on diurnal cycles (Bucci et al., 2005; Donovan et al., 2003; Kavanagh et al., 2007).

Darcy's Law can also be used to assess the combined hydraulic resistance of the SPAC components located proximally to the leaf, that is, between the soil and terminal branches ($R_{soil-branch}$). $R_{soil-branch}$ can be measured similarly to R_{total} by replacing Ψ_{leaf_md} with midday branch water potential (Ψ_{branch_md}) Then,

$$R_{soil-branch} = (\Psi_{soil} - \Psi_{branch\_md} - h\rho_w g)/F \qquad (3)$$

Ψ_{branch_md} is commonly measured with the pressure chamber technique on leaves that have been put into Ψ equilibrium with their proximal branches by stopping transpiration. This is achieved by sealing leaves in plastic bags and protecting the bags from solar radiation with reflective foil, usually for at least 1 h before the leaves are detached from the branch for measurement. This stops transpiration by placing the leaves in vapour-saturated air and closing stomata (Begg & Turner, 1970).

Since resistances in series are additive, that is, $R_{total} = R_{leaf} + R_{soil-branch}$, R_{leaf} can be calculated by combining Equations 1, 2, and 3 to give

$$R_{leaf} = (\Psi_{branch\_md} - \Psi_{leaf\_md})/F \qquad (4)$$

Then, dividing Equation 4 by Equation 1 gives fR_{leaf}. Since F is assumed to be in steady state within the SPAC, the equation simplifies (Equation 5), producing an estimate of fR_{leaf} without the need for F measurements and laboratory based K_{leaf} measurements.

$$fR_{leaf} = (\Psi_{branch\_md} - \Psi_{leaf\_md})/(\Psi_{leaf\_pd} - \Psi_{leaf\_md}) \qquad (5)$$

2.2 | Tropical tree fR_{leaf} field measurements

We measured fR_{leaf} in trees at two sites in central Panama where the Smithsonian Tropical Research Institute operates cranes that each access the canopy of ca.8000 m^2 of the forest. One site is in a seasonally dry tropical forest on the Pacific side of the isthmus in the Parque Natural Metropolitano that averages 1850 mm of rainfall annually with a dry season from December through April (Pivovaroff et al., 2021). The other site is in a wet tropical forest in the Bosque Protector San Lorenzo on the Caribbean side of the isthmus that averages 3300 mm of rainfall annually with a dry season from January through March (Pivovaroff et al., 2021).

We measured nine trees at each site, each of a different species (Supporting Information: Table S1). We selected canopy trees that were exposed to full sunlight and supported few or no lianas. Diameter at breast height (dbh) and height of the focal trees ranged 19–132 cm and 17–39 m, respectively (Supporting Information: Table S1).

Seven measurement campaigns were conducted at Parque Natural Metropolitano between 14 March 2016 and 13 June 2017 and 11 measurement campaigns were conducted in San Lorenzo between 21 March 2017 and 12 November 2018. During each campaign, we measured Ψ_{leaf} on mature sun-exposed upper-canopy leaves with a pressure chamber (PMS Instruments; precision ± 0.05 MPa). At predawn (05:00–6:30 h) and midday (11:30–13:00 h), we measured 2–3 leaves for Ψ_{leaf_pd} and Ψ_{leaf_md}, respectively. In addition, we sealed leaves in plastic bags and covered them with reflective foam insulation at predawn (04:00–05:00 h). At least one hour later, 2–3 covered leaves were measured for predawn branch water potential (Ψ_{branch_pd}) and at midday 2–3 covered leaves were measured for Ψ_{branch_md}. On each measurement day, we averaged values to obtain Ψ_{leaf_pd}, Ψ_{leaf_md}, Ψ_{branch_pd}, and Ψ_{branch_md} for each tree and then computed fR_{leaf} with Equation 5. Three of the 133 fR_{leaf} datapoints from these trees were outliers (i.e., >3 SD from the mean; Supporting Information: Figure S1) and were excluded from the tree-level mean fR_{leaf}.

On four of the measurement campaigns at each crane site, we also measured in situ transpiration with a portable photosynthesis machine (LI-6400XT, LI-COR Inc.) on 6–8 leaves that were also measured for Ψ_{leaf_md} between 10:00 and 15:00 h. We set cuvette conditions to closely match ambient conditions. Further details of the transpiration and Ψ_{leaf_md} measurements are described in Wu et al. (2020), Ely et al. (2022), Rogers et al. (2022), and Wolfe et al. (2022). We combined these with the Ψ_{leaf_pd} measurements to calculate leaf-area-specific K_{total} (i.e., inverse of Equation 1).

2.3 | Temperate tree fR_{leaf} field measurements

We measured fR_{leaf} on three 5-year-old *Pinus taeda* (loblolly pine) trees planted in full sun at the Louisiana State University AgCenter Burden Experimental Station, located in Baton Rouge, Louisiana, USA, on 4 February 2021. The trees were 167–191 cm height and 2.0–2.1 cm dbh. On each tree, we measured Ψ_{leaf_pd}, Ψ_{leaf_md}, Ψ_{branch_pd}, and Ψ_{branch_md} as described above. Each Ψ was the average of five leaves. We used the measurements to compute fR_{leaf} for each tree with Equation 5. Each leaf that was measured for Ψ_{leaf_md} was measured for transpiration with a portable photosynthesis machine (LI-6400XT, Li-Cor Inc.) with cuvette conditions set to closely match ambient conditions. *P. taeda* leaves grow in fascicles of three needles (generally, rarely two, or four needles). For each transpiration measurement one fascicle was placed in the cuvette (6400-02B, Li-Cor Inc.). Afterwards, the fascicles were imaged with a flatbed scanner and their diameter was measured with ImageJ. Leaf area was calculated from fascicle diameter following Blazier et al. (2018) and transpiration was scaled to leaf area. Then the inverse of Equation 1 was used to calculate K_{total} for each tree.

We measured fR_{leaf} on three *Persea borbonia* (red bay) trees growing in the forest understory at the margins of bayheads (i.e., stream bottoms) and pine forests at the H. G. Lee Memorial Forest in Washington Parish, Louisiana, USA, on 30 March 2021. The trees

were 1.5–1.7 m tall and 1.4–1.5 cm dbh. On each tree, we measured Ψ_{leaf_pd} and Ψ_{leaf_md}, Ψ_{branch_pd}, and Ψ_{branch_md} as described above. Each Ψ was the average of five leaves. We used the measurements to compute fR_{leaf} for each tree with Equation 5 and took the species-level mean.

2.4 | fR_{leaf} literature review

We used Web of Science, Google Scholar, and citations within publications to search for studies that reported Ψ_{leaf_pd}, Ψ_{leaf_md}, and Ψ_{branch_md} to compute fR_{leaf}. We excluded shrubs, tree seedlings (defined here as <1 m height), and potted plants. Only publications that concurrently measured all three components of Equation 5 (i.e., Ψ_{leaf_pd}, Ψ_{leaf_md}, and Ψ_{branch_md}) were included. For studies that reported values in figures but not in tables or text, we extracted the values using Web Plot Digitizer (Rohatgi, 2020). We took mean values of fR_{leaf} for species within each study unless the trees were measured under various conditions within a study (e.g., different habitats or experimental treatments), then we took the mean for each condition.

Combined with data that we collected (described above), we compiled 101 values of fR_{leaf} for 99 tree species (Supporting Information: Table S1). Among the samples, 36 included a measurement of Ψ_{branch_pd}. We used these to test the assumption of Ψ_{branch_pd}–Ψ_{leaf_pd} equilibrium by fitting an SMA through the points (Supporting Information: Figure S2). Disequilibrium between these values would indicate a pressure difference that violates the assumption of Ψ_{soil}–Ψ_{leaf_pd} equilibrium in Equation 2. Samples from temperate forests, tropical seasonal forests, and tropical rainforests did not vary from the 1:1 line, indicating equilibrium. However, samples from tropical savannas were above the 1:1 line, indicating a predawn pressure difference. Indeed, Bucci et al. (2005), reported Ψ_{soil}–Ψ_{leaf_pd} disequilibrium in this system due to nocturnal transpiration. Therefore, we excluded the 11 tropical savanna fR_{leaf} values (Supporting Information: Table S1) from our analyses.

To assess the allometric relationship between K_{total} and K_{leaf} with a data set that was expanded from Sack et al. (2003), we searched the literature as described above for studies that reported K_{total} and K_{leaf}. We found 19 paired values of K_{total} and K_{leaf} from 12 tree species across 5 studies (Supporting Information: Table S2). Note that K_{leaf} was measured in the laboratory on detached leaves, independently of K_{total}. Since K_{leaf} is generally considered a species-level trait (Scoffoni & Sack, 2017), we also paired K_{leaf} and K_{total} from disparate studies that measured only one of them on the same species. This produced a much larger sample size, 50 additional K_{leaf}–K_{total} pairs (Supporting Information: Table S2). However, compared to the K_{leaf}–K_{total} pairs from single studies, the pairs from disparate studies had higher variance (i.e., lower R^2) and a higher intercept (Supporting Information: Figure S3). K_{leaf}–K_{total} pairs from single studies are likely more reliable since K_{leaf} can vary within species among sites (Taneda et al., 2016), so we present only the analyses of K_{leaf}–K_{total} pairs from single studies.

2.5 | Data analysis

Before testing for differences in fR_{leaf} among biomes and between tree clades, we noted that fR_{leaf} was negatively related to tree height. Therefore, to test for differences in fR_{leaf} among biomes and between clades, we used ANCOVA with tree height as a covariate. Seven samples did not have values of tree height and were excluded from these analyses (Supporting Information: Table S1). To test whether fR_{leaf} was associated with Ψ_{branch_md}, Ψ_{leaf_pd}, and Ψ_{leaf_md}, we used Spearman's rank correlation analysis. Spearman's was used instead of Pearson's correlation analysis because variables were nonlinearly related. These correlations were confounded by the component variables appearing in both the x and y-axes, a statistical nuisance called the shared variables problem. To account for this, we compared the observed Spearman's correlation coefficients (r_s) to null correlations created with randomisation tests (Jackson & Somers, 1991). We randomly sampled without replacement the component variable from all observations and, along with the other two components, calculated fR_{leaf} with Equation 5. We then calculated r_s between the component variable and fR_{leaf} with the randomized data. This procedure was repeated 1000 times to create the null correlation. We then used z-tests to compute the p value ($\alpha = 0.05$) for the observed r_s in relation to the r_s obtained in the randomisation test.

To assess fR_{leaf} among the 19 paired values of K_{total} and K_{leaf} (Supporting Information: Table S2), we followed Sack et al. (2003). We fit an SMA through log_{10}-transformed values and interpreted the mean fR_{leaf} as the inverse of 10 to the power of the intercept. Additionally, we used the *smatr* package in R (Warton et al., 2012) to test for differences in the intercept, slope, and position along a common axis among biomes and tree clades.

3 | RESULTS

Among the samples measured with the in situ method using Equation 5, the mean fR_{leaf} was 0.51 (standard deviation [SD] = 0.24; 95% CI = 0.46–0.57) and fR_{leaf} declined with tree height ($R^2 = 0.30$, $P = 8e-8$; Figure 2). When four samples of conifer trees that were outliers in terms of height in the temperate forest (Figure 2) were excluded from the regression analysis, the result of declining fR_{leaf} with tree height remained ($R^2 = 0.23$, $P = 4e-6$). Although tree height differed among biomes (Figure 3a), fR_{leaf} did not differ among biomes ($F_{(2, 77)} = 0.89$, $p = 0.41$) or clades ($F_{(1, 79)} = 0.35$, $p = 0.56$) (Figures 2, 3b). fR_{leaf} was strongly correlated with Ψ_{branch_md} ($r_s = 0.61$) and, to a lesser extent, Ψ_{leaf_pd} ($r_s = 0.41$), while Ψ_{leaf_md} was not correlated with fR_{leaf} ($r_s = -0.04$) (Figure 4a,c,e). The correlation between fR_{leaf} and Ψ_{branch_md} was not any stronger than expected by random chance (Figure 4f) while the correlation between fR_{leaf} and Ψ_{leaf_pd} was significantly greater than expected by random chance (Figure 4b).

The SMA that was fit on paired K_{leaf}–K_{total} values showed an isometric relationship with a mean fR_{leaf} of 0.40 (95% CI = 0.29–0.56)
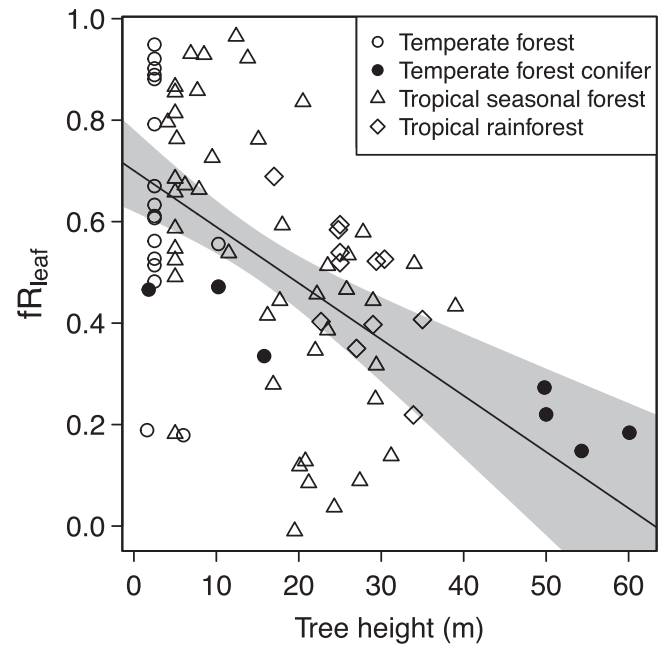
FIGURE 2 fR_{leaf} as a function of tree height. Points represent species or species by treatment combinations (Supporting Information: Table S1). The line represents a least squares linear regression fit through all the points, fR_{leaf} = 0.70 (SE = 0.041) −0.011 (SE = 0.002) × tree height. $R^2 = 0.30$. Shading represents the 95% confidence interval.
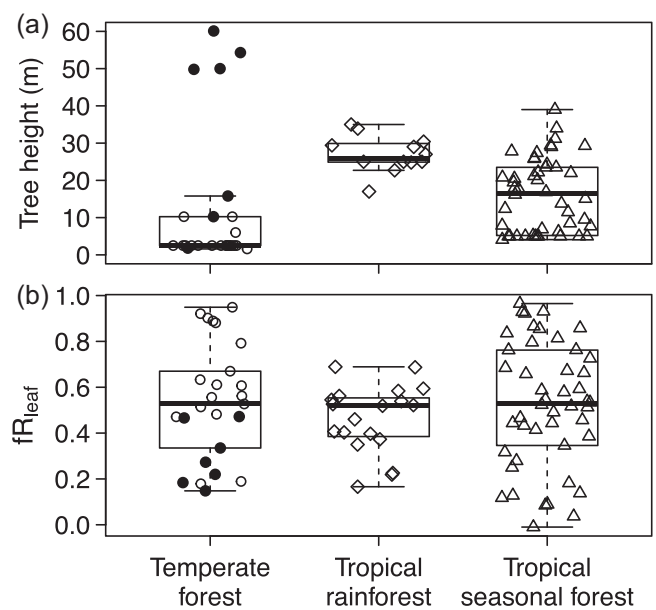
FIGURE 3 Distribution of measured tree heights (a) and fR_{leaf} values (b) among forest biomes. Boxes extend to the 25th and 75th quartiles and are bisected by the median. Bars extend to the most extreme data point that is no more than 1.5 times the length of the box away from the box. Points represent samples of species or species by treatment combinations (Supporting Information: Table S1). Symbols are drawn as in Figure 2.
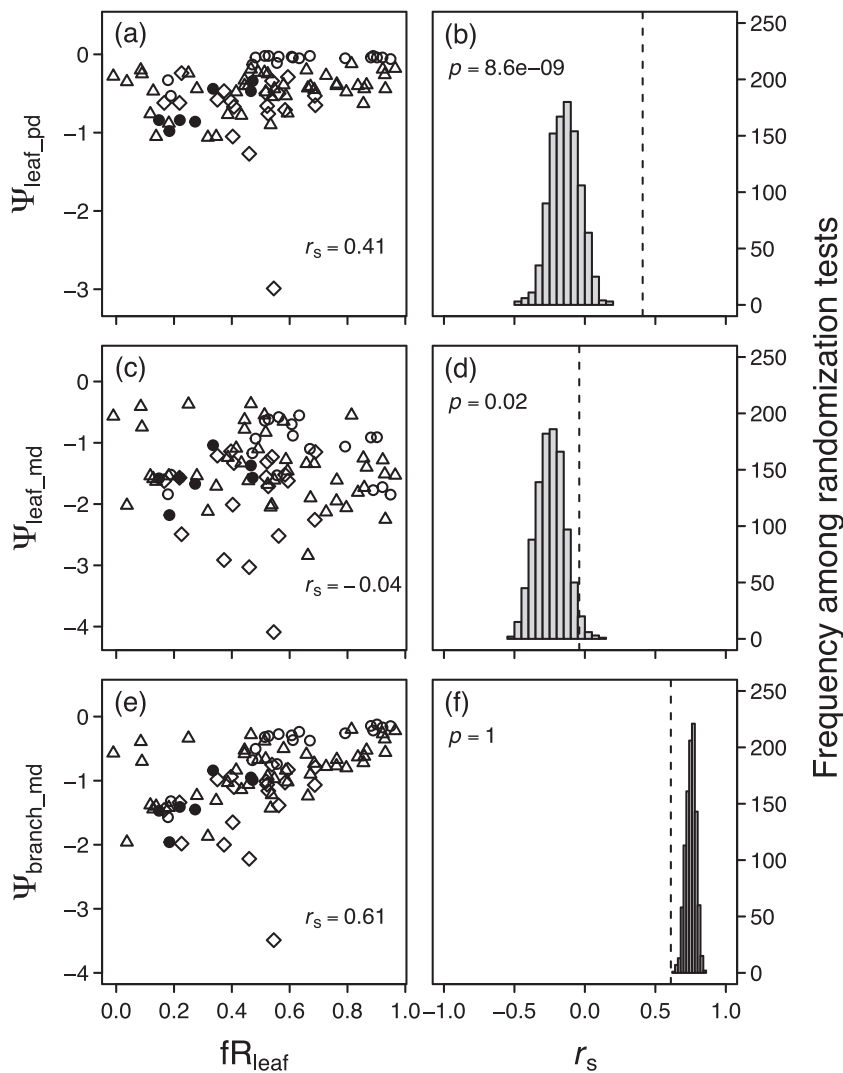
FIGURE 4 Relationships between fR_{leaf} and its component variables from Equation 5 (a, c, e). Symbols are drawn as in Figure 2. The Spearman's correlation coefficient (r_s) is shown in (a, c, e). Because the variables in these correlations are not independent, we used randomisation to test observed r_s against null values (b, d, f). Vertical dashed lines show the position of the observed r_s in relation to the frequency of r_s values from randomisation tests. p values indicate the probability of encountering an r_s equal to or greater than the observed r_s, using the randomisation tests for the null model.

(Figure 5). Among biomes, the SMA slope did not differ (likelihood ratio = 3.5, $p = 0.06$), but the intercept did (Wald = 10.1, $p = 0.002$). The intercept was larger for the tropical seasonal forest biome (0.57, 95% CI = 0.35−0.79; $fR_{leaf} = 0.27$, 95% CI = 0.16−0.45) than for the temperate forest biome (0.30, 95% CI = 0.13−0.48; $fR_{leaf} = 0.50$, 95% CI = 0.34−0.74). Comparisons between conifers and angiosperms found no differences in slope (likelihood ratio = 0.06, $p = 0.81$) or intercept (Wald = 0.96, $p = 0.33$), but conifers had lower K_{leaf} and K_{total} values than angiosperms along the common SMA line (Wald = 42.6, $P = 6e-11$).

4 | DISCUSSION

4.1 | fR_{leaf} is high and variable

Our multibiome assessment of in situ measurements found a mean fR_{leaf} of 0.51 among trees (Figures 3, 4). This value for trees is double the commonly cited value of 0.25 that Sack et al. (2003) presented for K_{total}−K_{leaf} allometry across multiple plant forms. However, it is

relatively similar to the fR_{leaf} of 0.45 obtained from the 11 trees and shrubs within the Sack et al. (2003) data set (see Introduction) and the fR_{leaf} of 0.40 obtained from the 19 trees in our expanded K_{total}−K_{leaf} allometry data set (Figure 5). Overall, these results suggest that fR_{leaf} is considerably higher among trees than seedlings and herbs. fR_{leaf} may be higher in trees because their roots and stems contain proportionally more secondary xylem than those of seedlings and herbs. Anatomical features in secondary xylem enable higher hydraulic conductance than in primary xylem (Evert, 2006) and proportionally higher hydraulic conductance in roots and stems would increase fR_{leaf}.

Among trees, the in situ method produced a higher mean fR_{leaf} than the K_{total}−K_{leaf} allometric method. This is likely because the in-situ method inherently accounts for dynamic K_{leaf} by measuring leaf and branch pressure differences simultaneously. In contrast, the K_{total}−K_{leaf} allometric method based on measurements of excised organs assumes that K_{leaf} measured in the laboratory is equal to K_{leaf} when K_{total} is measured in situ. However, K_{leaf} is dynamic on diurnal and seasonal time scales in association with multiple factors including Ψ_{leaf}, transpiration, and environmental conditions (Johnson
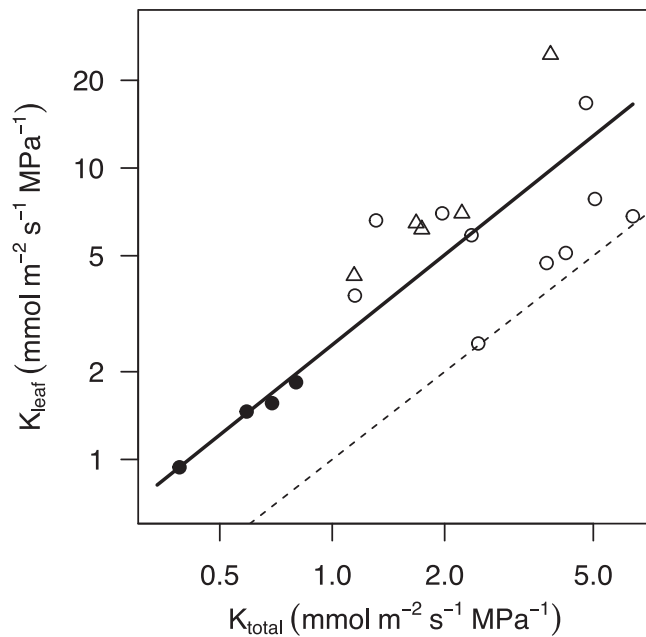
FIGURE 5 Allometric relationship between total hydraulic conductance (soil to leaf; K_{total}) and leaf hydraulic conductance (K_{leaf}). Each circle represents a tree species or species by treatment combination (Supporting Information: Table S2). Circles and triangles represent samples from temperate and tropical seasonal forests, respectively. Filled symbols represent conifers and open symbols represent angiosperms. The dashed 1:1 is shown for reference. The solid line represents a standardized major axis fit through all points. $Log_{10}(K_{leaf}) = 1.03$ (95% CI = 0.75–1.40) × K_{total} + $Log_{10}(2.47$; 95% CI = 1.77–3.45). $R^2 = 0.62$. Note that both axes are log scaled. CI, confidence interval.

et al., 2009, 2018; Sack & Holbrook, 2006; Simonin et al., 2015; Zhang et al., 2016). Our K_{total}–K_{leaf} allometric analysis and that of Sack et al. (2003) used maximum K_{leaf} obtained under laboratory conditions. This approach lowers the apparent fR_{leaf} if in situ K_{leaf} is lower than laboratory maximum K_{leaf}, which is common. For this reason, the in situ method likely produces a more accurate descriptor of fR_{leaf}.

fR_{leaf} obtained with the in-situ method was highly variable among samples, with SD = 0.24. This result contrasts with the expectation that fR_{leaf} is consistent among trees (e.g., De Cáceres et al., 2021; Wolfe et al., 2016). The wide range of fR_{leaf} values also calls into question the rule of thumb that hydraulic resistance is consistently partitioned between roots and shoots in a 50–50 split (e.g., Sperry et al., 1998). Our modelling exercise demonstrates how fR_{leaf} can vary within trees in response to environmental conditions and how this response depends on the leaf hydraulic vulnerability relative to other SPAC components (Figure 1d). Measured values of leaf and stem Ψ_{50} show a wide range of relative vulnerability; for example, among 63 angiosperm species the R^2 between leaf Ψ_{50} and stem Ψ_{50} was only 0.16 (Scoffoni & Sack, 2017). Hydraulic conductance of all SPAC components (i.e., soil, roots, stems, and leaves) is highly variable in response to environmental conditions (Domec et al., 2006, 2010, 2021; Johnson et al., 2009). Therefore, it is likely

that fR_{leaf} is not a reliable species-level trait, but rather is dependent on current and past environmental conditions experienced by individual trees.

4.2 | fR_{leaf} declines with tree height

We found that taller trees tend to have lower fR_{leaf} (Figure 2). This result is consistent with the results of von Allmen et al. (2015), who modelled fR_{leaf} in oak and maple trees and found that fR_{leaf} decreased as stem diameter increased. For maple and oak, respectively, they found fR_{leaf} decreased from 0.42 to 0.19 and from 0.36 to 0.17 among trees with trunk diameters 5 to 30 cm. This pattern could result through several processes. If K_{leaf} remains constant with tree height and K_{total} declines with tree height due to the increasing pathlength, this would result in a decrease of fR_{leaf} with tree height. Hydraulic conduit tapering can partially compensate for the effect of increasing pathlength but is unlikely, in itself, to prevent a decline in K_{total} (Savage et al., 2010; Zaehle, 2005). Indeed, among the trees in our analysis for which we had height and K_{total} data (Supporting Information: Table S2), we found no relationship between the two traits for angiosperms but a declining K_{total} with tree height for conifers (Supporting Information: Figure S4).

All else being equal, trees with higher leaf area to sapwood area ratios would have lower fR_{leaf} since leaves are arranged on branches analogously to resistors in parallel. In other words, as the leaf area to sapwood area ratio increases, hydraulic conductance in roots and stems is partitioned into smaller portions for each leaf, which corresponds to a lower fR_{leaf}. Yet, taller trees tend to have lower leaf area to sapwood area ratios (McDowell et al., 2002), which would have an effect in the opposite direction of our result of decreasing fR_{leaf} with tree height. However, as von Allmen et al. (2015) noted, as long as K_{total} declines with height faster than the leaf area to sapwood area ratio, then fR_{leaf} will decline with height. It is also possible that K_{leaf} declines with tree height (Zhang et al., 2009), which would counteract the effect of K_{total} decline with tree height. The relationship between height, fR_{leaf}, and these competing influences is likely highly variable among trees.

4.3 | fR_{leaf} as hydraulic protection

fR_{leaf} was positively correlated with Ψ_{branch_md} (Figure 4e). This result is predicted by the hydraulic segmentation hypothesis (Zimmermann, 1983) and our modelling exercise (Figure 1e). It suggests that fR_{leaf} can influence drought performance by preventing K_{stem} loss. However, because Ψ_{branch_md} and fR_{leaf} are not independent in our analyses (Equation 5), the correlation is susceptible to spuriousness (Jackson & Somers, 1991), which was confirmed with a randomisation test (Figure 4f). Therefore, our results do not directly support the hydraulic segmentation hypothesis. To do so would require other experimental approaches in which fR_{leaf} is assessed independently of Ψ_{branch} buffering. A study of excised shoots found

that drought-tolerant trees have proportionally higher R_{leaf} than drought-sensitive trees (Drake et al., 2015). Further, among arid-environment shrubs, K_{leaf} is positively correlated with the branch hydraulic safety margin (i.e., stem Ψ_{50} minus Ψ_{branch_md}) (Pivovaroff et al., 2014). However, direct evidence that high fR_{leaf} protects K_{stem} is lacking.

The finding that fR_{leaf} declined with Ψ_{leaf_pd} (Figure 4a) contrasts with our model prediction that fR_{leaf} remains relatively constant or increases as soil dries (Figure 1d). However, fR_{leaf} would be expected to decline with Ψ_{leaf_pd} if a nonleaf component contributed significantly to R_{total} and was more vulnerable than leaves. Roots and the rhizosphere likely follow this pattern (Bourbia et al., 2021; Rodriguez-Dominguez et al., 2018). The root-soil interface, root cortex and rhizosphere are generally very vulnerable to drying and can become hydraulic bottlenecks unless plants compensate by investing in sufficient absorptive root area (Cuneo et al., 2016; Lo Gullo et al., 1998; North et al., 2008; Rodriguez-Dominguez et al., 2018; Sperry et al., 2016). We explored how variation in rhizosphere hydraulic resistance interacts with fR_{leaf} to influence Ψ_{stem} buffering by comparing our simulations in Figure 1 with simulated soil dry downs where the average rhizosphere hydraulic resistance was set to 50% of average R_{total} (the default is 5%; Sperry et al., 2016) (Supporting Information: Figure S5). These simulations predicted reduced fR_{leaf} during initial Ψ_{soil} decline (Supporting Information: Figure S5d), consistent with observations (Figure 4a). Together, these results suggest that the influence of the root-soil interface, root cortex and rhizosphere on R_{total} increases as soil dries. In theory, upstream hydraulic vulnerability moderates fR_{leaf} buffering of Ψ_{stem}, but in any case, higher fR_{leaf} has higher Ψ_{stem} buffering capacity (compare Supporting Information: Figure 1e and S5e).

If hydraulic segmentation acts to protect stems, an important implication of declining fR_{leaf} with tree height (Figure 2) is that larger trees have less protection. Loss of K_{stem} is a key predictor of tree mortality during droughts (Adams et al., 2017). Large trees tend to suffer higher mortality rates than small trees during droughts (Bennett et al., 2015). In addition to other factors, including the higher VPD that larger trees experience (McDowell & Allen, 2015), lower fR_{leaf} may contribute to the trend for higher drought mortality in larger trees.

4.4 | Conclusions and limitations

Our literature review and field measurements combined data sets of Ψ_{leaf}, Ψ_{branch}, K_{total}, and K_{leaf} that were taken with varying techniques and sample sizes within and among trees and species (Supporting Information: Tables S1, S2). Ψ_{leaf} and Ψ_{branch} were often averaged over several days before they were input into Equation 5 to calculate fR_{leaf}. These discrepancies may have contributed to the high variation that we found in fR_{leaf} (Figures 2, 3). More standardized measurements with high replication are needed to better quantify fR_{leaf} and its variation within and among trees in association with plant traits

and in response to environmental conditions. Attention is also warranted to verify the assumptions in K_{total} and fR_{leaf} measurements: that Ψ_{leaf_pd} can quantify Ψ_{soil} in the rooting zone and that F is at steady state at midday. Our result of high mean fR_{leaf} suggests that leaf hydraulics play an even more outsized role in tree water relations than typically considered. Therefore, research focused on leaf hydraulics is likely to improve understanding of whole-plant water relations.

DATA AVAILABILITY STATEMENT

Upon publication, all data included in the manuscript will be made publicly available. The tropical data will be published in the NGEE Tropics Data Collection (https://ngt-data.lbl.gov/dois). The temperate data will be published in Zenodo (https://zenodo.org).

ORCID

Brett T. Wolfe http://orcid.org/0000-0001-7535-045X
Yong-Jiang Zhang http://orcid.org/0000-0001-5637-3015
Kristina J. Anderson-Teixeira http://orcid.org/0000-0001-8461-9713
Adam D. Collins http://orcid.org/0000-0001-9554-5190
L. Turin Dickman http://orcid.org/0000-0003-3876-7058
Kim S. Ely http://orcid.org/0000-0002-3915-001X
Adelodun R. Majekobaje http://orcid.org/0000-0003-3022-0891
Nate G. McDowell http://orcid.org/0000-0002-2178-2254
Sean T. Michaletz http://orcid.org/0000-0003-2158-6525
Alistair Rogers http://orcid.org/0000-0001-9262-7430
Shawn P. Serbin http://orcid.org/0000-0003-4136-8971
Zafar Siddiq http://orcid.org/0000-0002-1693-1649
Jin Wu http://orcid.org/0000-0001-8991-3970
Joseph Zailaa http://orcid.org/0000-0001-9103-190X
S. Joseph Wright http://orcid.org/0000-0003-4260-5676

REFERENCES

Adams, H.D., Zeppel, M.J.B., Anderegg, W.R.L., Hartmann, H., Landhäusser, S.M., Tissue, D.T. et al. (2017) A multi-species synthesis of physiological mechanisms in drought-induced tree mortality. *Nature Ecology & Evolution*, 1, 1285–1291.

Alarcón, J.J., Domingo, R., Green, S.R., Nicolás, E. & Torrecillas, A. (2003) Estimation of hydraulic conductance within field-grown apricot using sap flow measurements. *Plant and Soil*, 251, 125–135.

von Allmen, E.I., Sperry, J.S. & Bush, S.E. (2015) Contrasting whole-tree water use, hydraulics, and growth in a co-dominant diffuse-porous vs. ring-porous species pair. *Trees*, 29, 717–728.

Anderegg, W.R.L., Trugman, A.T., Badgley, G., Konings, A.G. & Shaw, J. (2020) Divergent forest sensitivity to repeated extreme droughts. *Nature Climate Change*, 10, 1091–1095.

Begg, J.E. & Turner, N.C. (1970) Water potential gradients in field tobacco. *Plant Physiology*, 46, 343–346.

Bennett, A.C., McDowell, N.G., Allen, C.D. & Anderson-Teixeira, K.J. (2015) Larger trees suffer most during drought in forests worldwide. *Nature Plants*, 1, 15139.

Blazier, M.A., Tyree, M.C., Sword Sayer, M.A., Kc, D., Hood, W.G. & Osbon, B.S. (2018) Gas exchange and productivity in temperate and droughty years of four eastern, elite loblolly pine genotypes grown in the Western gulf region. *International Journal of Agronomy*, 2018, 1–10.

Bourbia, I., Pritzkow, C. & Brodribb, T.J. (2021) Herb and conifer roots show similar high sensitivity to water deficit. *Plant Physiology*, 186, 1908–1918.

Brodribb, T.J., Holbrook, N.M. & Gutiérrez, M.V. (2002) Hydraulic and photosynthetic co-ordination in seasonally dry tropical forest trees. *Plant, Cell & Environment*, 25, 1435–1444.

Bucci, S.J., Goldstein, G., Meinzer, F.C., Franco, A.C., Campanello, P. & Scholz, F.G. (2005) Mechanisms contributing to seasonal homeostasis of minimum leaf water potential and predawn disequilibrium between soil and plant water potential in Neotropical savanna trees. *Trees*, 19, 296–304.

De Cáceres, M., Mencuccini, M., Martin-StPaul, N., Limousin, J.-M., Coll, L., Poyatos, R. et al. (2021) Unravelling the effect of species mixing on water use and drought stress in Mediterranean forests: a modelling approach. *Agricultural and Forest Meteorology*, 296, 108233.

Christoffersen, B.O., Gloor, M., Fauset, S., Fyllas, N.M., Galbraith, D.R., Baker, T.R. et al. (2016) Linking hydraulic traits to tropical forest function in a size-structured and trait-driven model (TFS v.1-Hydro). *Geoscientific Model Development*, 9, 4227–4255.

Cuneo, I.F., Knipfer, T., Brodersen, C.R. & McElrone, A.J. (2016) Mechanical failure of fine root cortical cells initiates plant hydraulic decline during drought. *Plant Physiology*, 172, 1669–1678.

Domec, J.-C., King, J.S., Carmichael, M.J., Overby, A.T., Wortemann, R.R., Smith, K.W. (2021) Root water gates and not changes in root structure provide new insights into plant physiological responses to drought, flooding and salinity. *Journal of Experimental Botany*, 72, 4489-4501.

Domec, J.-C., Noormets, A., King, J.S., Sun, G., Mcnulty, S.G., Gavazzi, M.J. et al. (2009) Decoupling the influence of leaf and root hydraulic conductances on stomatal conductance and its sensitivity to vapour pressure deficit as soil dries in a drained loblolly pine plantation. *Plant, Cell & Environment*, 32, 980–991.

Domec, J.-C., Schafer, K., Oren, R., Kim, H.S. & McCarthy, H.R. (2010) Variable conductivity and embolism in roots and branches of four contrasting tree species and their impacts on whole-plant hydraulic performance under future atmospheric CO2 concentration. *Tree Physiology*, 30, 1001–1015.

Domec, J.-C., Scholz, F.G., Bucci, S.J., Meinzer, F.C., Goldstein, G. & Villalobos-Vega, R. (2006) Diurnal and seasonal variation in root xylem embolism in neotropical savanna woody species: impact on stomatal control of plant water status. *Plant, Cell & Environment*, 29, 26–35.

Donovan, L.A., Richards, J.H. & Linton, M.J. (2003) Magnitude and mechanisms of disequilibrium between predawn plant and soil water potentials. *Ecology*, 84, 463–470.

Drake, P.L., Price, C.A., Poot, P. & Veneklaas, E.J. (2015) Isometric partitioning of hydraulic conductance between leaves and stems: balancing safety and efficiency in different growth forms and habitats. *Plant, Cell & Environment*, 38, 1628–1636.

Ely, K.S., Rogers, A., Wu, J., Wolfe, B.T., Dickman, L.T., Collins, A.D. et al. (2022) Leaf sample detail, Feb2016-May2016, PA-SLZ, PA-PNM, PA-BCI: Panama. 2. NGEE Tropics Data Collection. (dataset). https://doi.org/10.15486/ngt/1411971

Evert, R.F. (2006) *Esau's plant anatomy: Meristems, cells, and tissues of the plant body: their structure, function, and development*, 3rd Edition. Hoboken, New Jersey: Wiley-Interscience.

Fisher, R.A., Koven, C.D., Anderegg, W.R.L., Christoffersen, B.O., Dietze, M.C., Farrior, C.E. et al. (2018) Vegetation demographics in earth system models: a review of progress and priorities. *Global Change Biology*, 24, 35–54.

Goldstein, G., Andrade, J.L., Meinzer, F.C., Holbrook, N.M., Cavelier, J., Jackson, P. et al. (1998) Stem water storage and diurnal patterns of water use in tropical forest canopy trees. *Plant, Cell & Environment*, 21, 397–406.

Granier, A. (1985) Une nouvelle méthode pour la mesure du flux de sève brute dans le tronc des arbres. *Annales des Sciences Forestières*, 42, 193–200.

Jackson, D.A. & Somers, K.M. (1991) The spectre of "spurious" correlations. *Oecologia*, 86, 147–151.

Johnson, D.M., Berry, Z.C., Baker, K.V., Smith, D.D., McCulloh, K.A. & Domec, J.-C. (2018) Leaf hydraulic parameters are more plastic in species that experience a wider range of leaf water potentials. *Functional Ecology*, 32, 894–903.

Johnson, D.M., Woodruff, D.R., McCulloh, K.A. & Meinzer, F.C. (2009) Leaf hydraulic conductance, measured in situ, declines and recovers daily: leaf hydraulics, water potential and stomatal conductance in four temperate and three tropical tree species. *Tree Physiology*, 29, 879–887.

Kavanagh, K.L., Pangle, R. & Schotzko, A.D. (2007) Nocturnal transpiration causing disequilibrium between soil and stem predawn water potential in mixed conifer forests of Idaho. *Tree Physiology*, 27, 621–629.

Lo Gullo, M.A., Nardini, A., Salleo, S. & Tyree, M.T. (1998) Changes in root hydraulic conductance (KR) of Olea oleaster seedlings following drought stress and irrigation. *New Phytologist*, 140, 25–31.

Loustau, D., Domec, J.-C. & Bosc, A. (1998) Interpreting the variations in xylem sap flux density within the trunk of maritime pine (*Pinus pinaster* ait.): application of a model for calculating water flows at tree and stand levels. *Annales des Sciences Forestières*, 55, 29–46.

Maherali, H. & DeLucia, E.H. (2001) Influence of climate-driven shifts in biomass allocation on water transport and storage in ponderosa pine. *Oecologia*, 129, 481–491.

McDowell, N., Barnard, H., Bond, B., Hinckley, T., Hubbard, R., Ishii, H. et al. (2002) The relationship between tree height and leaf area: sapwood area ratio. *Oecologia*, 132, 12–20.

McDowell, N.G. & Allen, C.D. (2015) Darcy's law predicts widespread forest mortality under climate warming. *Nature Climate Change*, 5, 669–672.

Moreshet, S., Cohen, Y., Green, G.C. & FUC, M. (1990) The partitioning of hydraulic conductances within mature orange trees. *Journal of Experimental Botany*, 41, 833–839.

North, G.B., Brinton, E.K. & Garrett, T.Y. (2008) Contractile roots in succulent monocots: convergence, divergence and adaptation to limited rainfall. *Plant, Cell & Environment*, 31, 1179–1189.

Pearcy, R.W., Schulze, E.-D. & Zimmermann, R. (1989) Measurement of transpiration and leaf conductance. In: Pearcy, R.W., Ehleringer, J.,

Mooney, H.A. & Rundel, P.W. (Eds.) *In* Plant Physiological Ecology Field Methods and Instrumentation. London, UK: Chapman and Hall, pp. 137–160.

Pivovaroff, A.L., Sack, L. & Santiago, L.S. (2014) Coordination of stem and leaf hydraulic conductance in Southern California shrubs: a test of the hydraulic segmentation hypothesis. *New Phytologist*, 203, 842–850.

Pivovaroff, A.L., Wolfe, B.T., McDowell, N., Christoffersen, B., Davies, S., Dickman, L.T. et al. (2021) Hydraulic architecture explains species moisture dependency but not mortality rates across a tropical rainfall gradient. *Biotropica*, 53, 1213–1225.

Pratt, R.B., Jacobsen, A.L., Percolla, M.I., De Guzman, M.E., Traugh, C.A. & Tobin, M.F. (2021) Trade-offs among transport, support, and storage in xylem from shrubs in a semiarid chaparral environment tested with structural equation modeling. *Proceedings of the National Academy of Sciences*, 118, e2104336118.

Rodriguez-Dominguez, C.M., Carins Murphy, M.R., Lucani, C. & Brodribb, T.J. (2018) Mapping xylem failure in disparate organs of whole plants reveals extreme resistance in olive roots. *New Phytologist*, 218, 1025–1035.

Rogers, A., Serbin, S.P., Ely, K.S., Wu, J., Wolfe, B.T., Dickman, L.T. et al. (2022) Diurnal leaf gas exchange survey, Feb2016-May2016, PA-SLZ, PA-PNM: Panama. 2. NGEE Tropics Data Collection. (dataset). ps://doi.org/10.15486/ngt/1411972

Rohatgi, A. (2020) WebPlotDigitizer.

Sack, L., Cowan, P.D., Jaikumar, N. & Holbrook, N.M. (2003) The 'hydrology' of leaves: co-ordination of structure and function in temperate woody species. *Plant, Cell & Environment*, 26, 1343–1356.

Sack, L. & Holbrook, N.M. (2006) Leaf hydraulics. *Annual review of plant biology*, 57, 361–381.

Savage, V.M., Bentley, L.P., Enquist, B.J., Sperry, J.S., Smith, D.D., Reich, P.B. et al. (2010) Hydraulic trade-offs and space filling enable better predictions of vascular structure and function in plants. *Proceedings of the National Academy of Sciences*, 107, 22722–22727.

Scholz, F.G., Phillips, N.G., Bucci, S.J., Meinzer, F.C. & Goldstein, G. (2011) Hydraulic capacitance: biophysics and functional significance of internal water sources in relation to tree size. In: Meinzer, F.C., Lachenbruch, B. & Dawson, T.E. (Eds.) *In Size- and Age-Related Changes in Tree Structure and Function*. New York: Springer, pp. 341–362.

Schwalm, C.R., Anderegg, W.R.L., Michalak, A.M., Fisher, J.B., Biondi, F., Koch, G. et al. (2017) Global patterns of drought recovery. *Nature*, 548, 202–205.

Scoffoni, C. & Sack, L. (2017) The causes and consequences of leaf hydraulic decline with dehydration. *Journal of Experimental Botany*, 68, 4479–4496.

Simonin, K.A., Burns, E., Choat, B., Barbour, M.M., Dawson, T.E. & Franks, P.J. (2015) Increasing leaf hydraulic conductance with transpiration rate minimizes the water potential drawdown from stem to leaf. *Journal of Experimental Botany*, 66, 1303–1315.

Smith, D.D., Sperry, J.S., Enquist, B.J., Savage, V.M., McCulloh, K.A. & Bentley, L.P. (2014) Deviation from symmetrically self-similar branching in trees predicts altered hydraulics, mechanics, light interception and metabolic scaling. *New Phytologist*, 201, 217–229.

Sperry, J.S., Adler, F.R., Campbell, G.S. & Comstock, J.P. (1998) Limitation of plant water use by rhizosphere and xylem conductance: results from a model. *Plant, Cell and Environment*, 21, 347–359.

Sperry, J.S., Hacke, U.G., Oren, R. & Comstock, J.P. (2002) Water deficits and hydraulic limits to leaf water supply. *Plant, Cell & Environment*, 25, 251–263.

Sperry, J.S., Wang, Y., Wolfe, B.T., Mackay, D.S., Anderegg, W.R.L., McDowell, N.G. et al. (2016) Pragmatic hydraulic theory predicts stomatal responses to climatic water deficits. *New Phytologist*, 212, 577–589.

Taneda, H., Kandel, D.R., Ishida, A. & Ikeda, H. (2016) Altitudinal changes in leaf hydraulic conductance across five Rhododendron species in eastern Nepal. *Tree Physiology*, 36, 1272–1282.

Trugman, A.T., Anderegg, L.D.L., Wolfe, B.T., Birami, B., Ruehr, N.K., Detto, M. et al. (2019) Climate and plant trait strategies determine tree carbon allocation to leaves and mediate future forest productivity. *Global Change Biology*, 25, 3395–3405.

Tyree, M.T., Snyderman, D.A., Wilmot, T.R. & Machado, J.-L. (1991) Water relations and hydraulic architecture of a tropical tree (*Schefflera morototoni*): data, models, and a comparison with two temperate species (*Acer saccharum* and *Thuja occidentalis*). *Plant Physiology*, 96, 1105–1113.

Venturas, M.D., Sperry, J.S. & Hacke, U.G. (2017) Plant xylem hydraulics: what we understand, current research, and future challenges. *Journal of Integrative Plant Biology*, 59, 356–389.

Warton, D.I., Duursma, R.A., Falster, D.S. & Taskinen, S. (2012) SMATR 3 – an R package for estimation and inference about allometric lines. *Methods in Ecology and Evolution*, 3, 257–259.

Whitehead, D. (1998) Regulation of stomatal conductance and transpiration in forest canopies. *Tree Physiology*, 18, 633–644.

Wolfe, B.T., Sperry, J.S. & Kursar, T.A. (2016) Does leaf shedding protect stems from cavitation during seasonal droughts? A test of the hydraulic fuse hypothesis. *New Phytologist*, 212, 1007–1018.

Wolfe, B.T., Wu, J., Ely, K.S., Serbin, S.P., Rogers, A., Dickman, L.T.... Michaletz, S.T. (2022) Leaf water potential, Feb2016-May2016, PA-SLZ, PA-PNM, PA-BCI: Panama. NGEE Tropics Data Collection. (dataset). https://doi.org/10.15486/ngt/1507766

Wu, J., Serbin, S.P., Ely, K.S., Wolfe, B.T., Dickman, L.T., Grossiord, C. et al. (2020) The response of stomatal conductance to seasonal drought in tropical forests. *Global Change Biology*, 26, 823–839.

Zaehle, S. (2005) Effect of height on tree hydraulic conductance incompletely compensated by xylem tapering. *Functional Ecology*, 19, 359–364.

Zhang, Y.-J., Meinzer, F.C., Hao, G.-Y., Scholz, F.G., Bucci, S.J., Takahashi, F.S. et al. (2009) Size-dependent mortality in a Neotropical savanna tree: the role of height-related adjustments in hydraulic architecture and carbon allocation. *Plant, Cell & Environment*, 32, 1456–1466.

Zhang, Y.-J., Rockwell, F.E., Graham, A.C., Alexander, T. & Holbrook, N.M. (2016) Reversible leaf xylem collapse: a potential "circuit breaker" against cavitation. *Plant Physiology*, 172, 2261–2274.

Zimmermann, M.H. (1983) *Xylem structure and the ascent of sap*. Berlin: Springer-Verlag.

SUPPORTING INFORMATION

Additional supporting information can be found online in the Supporting Information section at the end of this article.